Beating Irregularity of Single Pacemaker Cells Isolated from the Rabbit Sinoatrial Node

Ronald Wilders and Habo J. Jongsma
Department of Physiology, University of Amsterdam, Amsterdam, The Netherlands

ABSTRACT Single pacemaker heart cells discharge irregularly. Data on fluctuations in interbeat interval of single pacemaker cells isolated from the rabbit sinoatrial node are presented. The coefficient of variation of the interbeat interval is quite small, ~2%, even though the coefficient of variation of diastolic depolarization rate is ~15%. It has been hypothesized that random fluctuations in interbeat interval arise from the stochastic behavior of the membrane ionic channels. To test this hypothesis, we constructed a single channel model of a single pacemaker cell isolated from the rabbit sinoatrial node, i.e., a model into which the stochastic open-close kinetics of the individual membrane ionic channels are incorporated. Single channel conductances as well as single channel open and closed lifetimes are based on experimental data from whole cell and single channel experiments that have been published in the past decade. Fluctuations in action potential parameters of the model cell are compared with those observed experimentally. It is concluded that fluctuations in interbeat interval of single sinoatrial node pacemaker cells indeed are due to the stochastic open-close kinetics of the membrane ionic channels.

GLOSSARY

Action potential parameters

APA	action potential amplitude (in millivolts)
APD_{50}	action potential duration at 50% repolarization (in milliseconds)
APD_{100}	action potential duration at 100% repolarization (in millisecond)
DDR	diastolic depolarization rate (in millivolts/second)
IBI	interbeat interval (in milliseconds)
MDP	maximum diastolic potential (in millivolts)
TOP	takeoff potential (in millivolts)
$\dot{V}_{max}$	maximum upstroke velocity (in volts/second)

Symbols and units

α_x, α_y, ...	rate constant of gating variable $x, y, \ldots$ (in milliseconds^{-1})
β_x, β_y, ...	rate constant of gating variable $x, y, \ldots$ (in milliseconds^{-1})
$\gamma_{Ca,L}$, $\gamma_{Ca,T}$, ...	single channel conductance of the $i_{Ca,L}$, $i_{Ca,T}$, ... channels (in picosiemens)
A_m	membrane area (in microns^2)
C_{IBI}	coefficient of variation of interbeat interval
C_m	membrane capacitance (in picofarads)
d_L	activation gating variable of $i_{Ca,L}$
d_T	activation gating variable of $i_{Ca,T}$
f_L	inactivation gating variable of $i_{Ca,L}$
f_T	inactivation gating variable of $i_{Ca,T}$
$\bar{g}_{Ca,L}$, $\bar{g}_{Ca,T}$, ...	fully activated conductance of $i_{Ca,L}$, $i_{Ca,T}$, ... (in nanosiemens)
h	inactivation gating variable of i_{Na}
$i_{Ca,L}$	L-type calcium current (in picoamperes)
$\bar{i}_{Ca,L}$, $\bar{i}_{Ca,T}$, ...	fully activated $i_{Ca,L}$, $i_{Ca,T}$, ... (in picoamperes)
$i_{Ca,T}$	T-type calcium current (in picoamperes)
i_f	hyperpolarizing-activated current (in picoamperes)
i_K	delayed rectifying potassium current (in picoamperes)
i_{Na}	fast sodium current (in picoamperes)
i_{tot}	net current crossing the membrane (in picoamperes)
m	activation gating variable of i_{Na}
$N_{Ca,L}$, $N_{Ca,T}$, ...	number of $i_{Ca,L}$, $i_{Ca,T}$, ... channels comprising the cell membrane
V_m	membrane potential (in millivolts)
x	activation gating variable of i_K
y	activation gating variable of i_f

INTRODUCTION

Starting with the original observations by Blair and Erlanger (1932), much attention has been paid to the apparently random firing behavior of the nerve membrane in response to near-threshold stimuli. Nevertheless, the mechanism underlying these fluctuations in membrane excitability remained obscure for many years. Experimental investigations of fluctuations in membrane potential of the excitable nerve membrane were initiated by Verveen and Derksen (see, e.g., Verveen and Derksen, 1965; Derksen and Verveen, 1966). In a theoretical study, Lecar and Nossal (1971a, b), performing specific calculations for the node of Ranvier of the frog, demonstrated that fluctuations in membrane conductance, associated with ionic channels that open and close randomly, might be the major source of membrane noise. The relationship between nerve membrane excitability and single channel open-close kinetics has been studied directly using

Received for publication 14 January 1993 and in final form 27 September 1993.

Address reprint requests to Ronald Wilders, Department of Physiology, University of Amsterdam, Meibergdreef 15, 1105 AZ Amsterdam, The Netherlands.

Dr. Wilders' and Dr. Jongsma's present address is Department of Medical Physiology and Sports Medicine, University of Utrecht, Vondellaan 24, 3521 GG Utrecht, The Netherlands.

0006-3495/93/12/2601/13 $2.00

a single channel model of the unclamped nerve membrane based upon the original Hodgkin and Huxley (1952) model (Skaugen and Walløe, 1979; Clay and DeFelice, 1983; DeFelice and Clay, 1983; van Meerwijk, 1988). The stochastic model comprises two extra parameters: the numbers of sodium and potassium channels in the membrane patch under consideration. These numbers may be inferred from estimates of channel densities or from estimates of single channel conductances.

Single pacemaker cells isolated from the rabbit sinoatrial (SA) node discharge irregularly (Fig. 1): their interbeat interval (IBI) shows random fluctuations about an ideal mean. Similar observations have been made in other preparations that display spontaneous beating, e.g., in small clusters of embryonic chick ventricular cells containing 1–125 cells (Clay and DeHaan, 1979), in single neonatal rat atrial and ventricular cells (Jongsma and Tsjernina, 1982), and in small groups of neonatal rat heart cells (Jongsma et al., 1983). Clay and DeHaan (1979) hypothesized that these random fluctuations in IBI, like the threshold fluctuations in nerve membrane, result from random opening and closing of membrane ionic channels. They constructed a simple model of random membrane voltage fluctuations superimposed on a linear depolarization from maximum diastolic potential to threshold. The membrane voltage noise needed to explain experimentally observed IBI fluctuations corresponded nicely to that extrapolated from steady-state noise recorded from resting heart cell aggregates. They noted, as did Clay and DeFelice (1983), that a more detailed model study of the relationship between IBI fluctuations and single channel open-close kinetics would require a complete set of voltage clamp data on heart cell membrane currents, to be obtained in whole cell as well as single channel experiments. Such experiments have now been carried out on single isolated rabbit SA node cells, yielding detailed information on conductance and kinetics of the L- and T-type calcium currents $i_{Ca,L}$ and $i_{Ca,T}$ (Hagiwara et al., 1988), the hyperpolarizing-activated current i_f (DiFrancesco, 1986; DiFrancesco et al., 1986; van Ginneken and Giles, 1991), and the delayed rectifying potassium current i_K (Shibasaki, 1987), which are believed to be the major

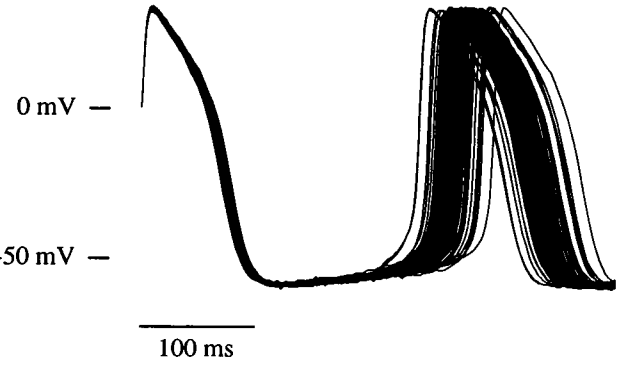

FIGURE 1 Beating irregularity of a single pacemaker cell isolated from the rabbit sinoatrial node, demonstrated by superimposing 100 consecutive action potentials that were recorded from cell 910108c2.

gated membrane currents in these cells (for a review, see Irisawa et al., 1993). These data were used when constructing our deterministic model describing the electrical activity of a single pacemaker cell isolated from the rabbit SA node (Wilders et al., 1991).

The aim of the present study was to investigate in detail the relationship between fluctuations in interbeat interval of single SA node pacemaker cells and the open-close kinetics of the membrane ionic channels. To this end, we constructed a stochastic model of electrical activity of a single isolated rabbit SA node cell based upon our deterministic model. Instead of adding noise to the differential equations, we allowed noise as a consequence of channel kinetics: single channel open and closed lifetimes were obtained from a probabilistic interpretation of the deterministic rate constants. The principles of this simulation technique have previously been set out by Skaugen and Walløe (1979), Clay and DeFelice (1983), DeFelice and Clay (1983), and van Meerwijk (1988). For each time-dependent (gated) membrane current, the number of channels was inferred from the fully activated conductance in the deterministic model and an estimate of the single channel conductance under normal physiological conditions.

Model results were compared with data from current clamp experiments on single isolated rabbit SA node cells that were carried out in our laboratory. The model was used to determine the contribution of each gated membrane current to fluctuations in interbeat interval and to study the relationship between fluctuations in interbeat interval and the number of ion channels in the cell membrane. This study has been published in preliminary form as part of a doctoral thesis (Wilders, 1993).

MATERIALS AND METHODS

Experiments

In a correlative study on electrical and morphological properties of single pacemaker cells isolated from the rabbit SA node, trains of ~100 action potentials were recorded in our laboratory by E. E. Verheijck, A. C. G. van Ginneken, and L. N. Bouman. Their experimental methods will be described in detail elsewhere (manuscript in preparation). In brief, cells were enzymatically dissociated from the SA nodal region of hearts of 1.8–2.5-kg New Zealand albino rabbits according to the method of DiFrancesco et al. (1986), with some modifications. For single cell recordings, both "spindle" and "elongated spindle" cells (Verheijck et al., 1992) were used. The membrane potential of these pacemaker cells was recorded using either the whole cell patch clamp technique (Hamill et al., 1981) or the perforated patch clamp technique (Horn and Marty, 1988), in the current clamp mode. All experiments were performed at 35 ± 0.5°C. Action potential parameters (see "Glossary") were measured using a custom-written program that was run in a LabVIEW software environment (National Instruments Corporation, Austin, TX) on a Macintosh IIci computer (Apple Computer, Inc., Cupertino, CA).

Before any further analysis, we inspected the action potential parameters for apparent artifacts such as, e.g., a beat-to-beat decrease in action potential amplitude or a sudden increase in maximum diastolic potential, associated with "rundown" and recording pipette instabilities, respectively. If such artifacts, which may have considerable effects on the fluctuations in interbeat interval, were detected, the experiment was discarded.

Action potential parameters

Unlike other action potential parameters (see "Glossary"), there are no universally accepted definitions of diastolic depolarization rate (DDR) and takeoff potential (TOP). We defined the DDR as $\Delta V_m/\Delta t$, where ΔV_m is the change in membrane potential during a 150-ms time interval, i.e., $\Delta t = 150$ ms, starting at a membrane potential that is 1 mV positive to the maximum diastolic potential (MDP) (Fig. 2 *A*). For cells with a short mean diastolic time, e.g., cell 910108c2 (Fig. 1), Δt was set to 100 instead of 150 ms. The TOP was defined as the membrane potential at which dV_m/dt equals the average rate of rise of the action potential from MDP + 1 mV to its overshoot potential (Fig. 2 *B*).

Numerical computations

We applied the first order numerical integration method of Victorri et al. (1985) to calculate the variation of the membrane potential V_m during pacemaker activity. The algorithm of Wichmann and Hill (1982) was used to obtain random numbers from the uniform distribution on (0,1).

The integration time step Δt was selected as follows. Having arrived at time t, consecutive lifetimes, T, of the membrane state are drawn according to

$$T = (-\log r)/\lambda, \quad (1)$$

where r is a random number between 0 and 1, and λ is the sum of all appropriate rate constants, i.e., α_q for each closed q gate and β_q for each open q gate, until an instantaneous jump in membrane conductance, brought about by an opening or a closure of a single channel, occurs. Next, these consecutive lifetimes are added up to give Δt. Note that the lifetime probability distribution, being dependent on the state of each channel through the parameter λ (Eq. 1), changes after each drawing of a particular membrane state lifetime. Once Δt is known, Eq. 5 is integrated to give V_m at the new time $t + \Delta t$, and new values for all α's, β's, and i's are calculated, allowing the next Δt to be selected.

On the rare occasion that Δt exceeds the maximum value Δt_{max}, which equals one of the values $2^n \cdot 0.032$ ms, $0 \leq n \leq 5$, depending on V_m, and is taken from the deterministic model (Wilders et al., 1991), Δt is set equal to Δt_{max} without a change in membrane state at time $t + \Delta t$. Because our system, based on Markov processes, lacks memory, this operation does not affect the probability distribution of the lifetime of the latter membrane state.

The stochastic model was translated into a FORTRAN program that was run on a VAX 4000–300 computer (Digital Equipment Corporation, Maynard, MA) or an ES/9000–720 computer (International Business Machines Corporation, Armonk, NY). Calculations were carried out with a degree of precision of ~16 decimal figures.

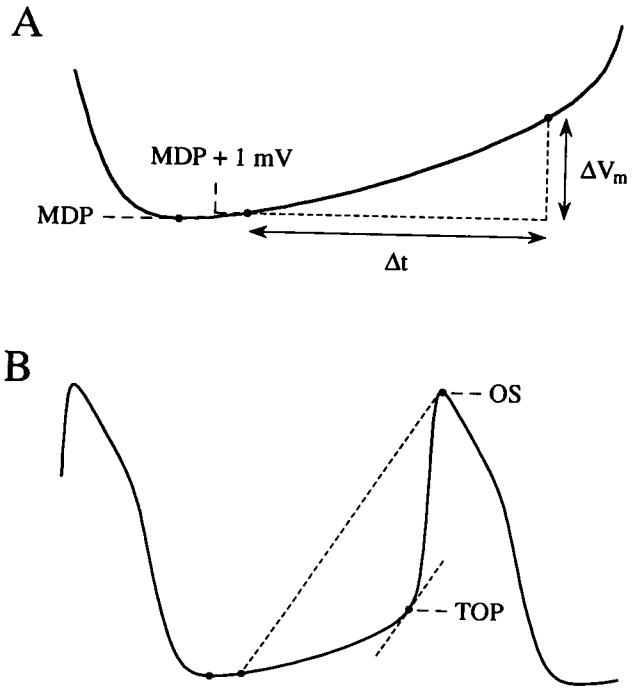

FIGURE 2 Definition of the action potential parameters DDR and TOP. (*A*) The DDR is defined as $\Delta V_m/\Delta t$, where ΔV_m is the change in membrane potential during the time interval Δt, starting at a membrane potential 1 mV positive to MDP. Δt is set to 100 or 150 ms, depending on the mean diastolic time of the cell. (*B*) The TOP is defined as the membrane potential at which the slope of the action potential equals the average rate of rise of the action potential from MDP + 1 mV to its overshoot potential (*OS*).

STOCHASTIC MODEL

Time-dependent (gated) membrane currents

Five gated membrane currents are involved in the pacemaker activity of our model cell: $i_{Ca,L}$, $i_{Ca,T}$, i_f, i_K, and i_{Na}. Gating of the $i_{Ca,L}$ channels is controlled by a fast activation gate, the d_L gate, and a slower inactivation gate, the f_L gate. The L-type calcium current contributes significantly to the last part of the diastolic depolarization and the upstroke of the action potential. Similarly, gating of the $i_{Ca,T}$ channels is controlled by a fast activation gate, the d_T gate and a somewhat slower inactivation gate, the f_T gate. The contribution of the T-type calcium current to pacemaking is small and is limited to the last part of diastolic depolarization. The kinetics of the i_f channels are described with two identical slow activation gates, the y gates. The hyperpolarizing activated current contributes significantly to diastolic depolarization. Gating of the i_K channels is controlled by a single, rather slow activation gate, the x gate. The delayed rectifying potassium current contributes significantly to the repolarization of the action potential. The fast sodium current, i_{Na}, has not consistently been found in SA nodal pacemaker cells. In the model, its kinetics are described with three identical very fast activation gates, the m gates, and a single, slower inactivation gate, the h gate. The behavior of i_{Na} is quite similar to that of $i_{Ca,T}$, and, thus, contributes little to diastolic depolarization.

Model assumptions

We assume that each gate flips randomly between two states: the "open state" and the "closed state." Then, a particular open lifetime, T_o, can be obtained by drawing a random number r from the uniform distribution on (0,1) and calculating T_o from

$$T_o = (-\log r)/\beta. \quad (2)$$

Similarly, a particular closed lifetime, T_c, is given by

$$T_c = (-\log r)/\alpha, \quad (3)$$

where α and β are the Hodgkin and Huxley (1952) type rate constants of the deterministic model (Skaugen and Walløe, 1979; Clay and DeFelice, 1983; DeFelice and Clay, 1983).

In addition, we will make the following assumptions. (*a*) Each gated membrane current flows through specific, identical channels. (*b*) A channel is conducting only if all of its gates are in their open state. Thus, each channel has one open state and one or more closed states. (*c*) Gates or channels do not interact. (*d*) There are no regional differences in membrane potential.

Stochastic behavior of the membrane conductance

In the deterministic model, the membrane conductance state is determined by the continuous Hodgkin and Huxley (1952) type gating variables $d_L, f_L, d_T, f_T, y, x, m$, and h, each ranging between 0 and 1, and obeying the first-order differential equation

$$dq/dt = \alpha_q(1 - q) - \beta_q q, \quad (4)$$

where q denotes the gating variable. In the stochastic model, the membrane state is determined by the discrete numbers of channels in open and closed states. Using Eqs. 2 and 3 to draw open and closed lifetimes of single gates, it is a rather straightforward operation to incorporate the stochastic behavior of individual gated ion channels into the deterministic model of the free-running, non-voltage-clamped cell membrane (Skaugen and Walløe, 1979; Clay and DeFelice, 1983; DeFelice and Clay, 1983; van Meerwijk, 1988; Wilders, 1993).

If all gated membrane currents are described stochastically, a drawing procedure yielding membrane state lifetimes replaces the integration of the Eq. 4-like differential equations for the gating variables. Then, the only differential equation left over from the deterministic model, apart from the differential equations describing changes in intracellular ion concentrations, is

$$dV_m/dt = -i_{tot}/C_m. \quad (5)$$

Simplification of i_{Na} kinetics

The fast kinetics of the m gates of the i_{Na} channels, inducing numerous transitions between different closed states per integration time step, substantially reduce the speed of computation. Hypothesizing that these transitions hardly affect fluctuations in action potential parameters, we applied the stochastic approach to i_{Na} channels with all m gates open only (cf. Skaugen and Walløe, 1979). We verified that this simplification did not affect model results. Hence, all simulations presented here were carried out with simplified i_{Na} kinetics.

Estimation of the number of channels

If a gated membrane current is described stochastically, the number of single channels carrying this current, N, becomes a parameter of the model. This number can be calculated by dividing the fully activated conductance $\bar{g}$, taken from the deterministic model, by the single channel conductance γ. We can only estimate this single channel conductance, because, up to now, all experiments yielding single channel conductances have been carried out under rather unphysiological conditions, e.g., at low temperature or with a high charge carrier concentration to increase the signal/noise ratio. A summary of single channel conductances observed in patch clamp experiments on mammalian cardiac myocytes is given in Table 1.

Number of $i_{Ca,L}$ channels

In rabbit SA node cells, Hagiwara et al. (1988) observed a $\gamma_{Ca,L}$ of 16 pS at 37°C, the extracellular solution containing 100 mM Ba^{2+} as the charge carrier. In guinea pig ventricular cells, Cavalié et al. (1983) observed values of $\gamma_{Ca,L}$ at 50 and 90 mM Ba^{2+}, the value at 50 mM Ba^{2+} being 50–60% of the value at 90 mM Ba^{2+} (Table 1). If the same ratio holds true

Table 1 Single channel conductances observed in patch clamp experiments on mammalian cardiac myocytes

	Preparation	Single Channel Conductance (pS)	Temperature (°C)	Extracellular Solution (mM)
L-type calcium channels				
Cavalié et al. (1983)	Guinea pig ventricle	10	30–32	50 Ba^{2+}
Cavalié et al. (1983)	Guinea pig ventricle	18	30–32	90 Ba^{2+}
Cavalié et al. (1983)	Guinea pig ventricle	9	30–32	50 Ca^{2+}
Hagiwara et al. (1988)	Rabbit sinoatrial node	16	37	100 Ba^{2+}
Reuter et al. (1982)	Neonatal rat heart	25	24–26	96 Ba^{2+}
T-type calcium channels				
Droogmans and Nilius (1989)	Guinea pig ventricle	6.8	22 ± 1	110 Ca^{2+}
Hagiwara et al. (1988)	Rabbit sinoatrial node	8.5	37	100 Ba^{2+}
Nilius et al. (1985)	Guinea pig ventricle	8	21	110 Ba^{2+}
i_f Channels				
DiFrancesco (1986)	Rabbit sinoatrial node	0.98	35–36	70 K^+, 70 Na^+
Sodium channels				
Cachelin et al. (1983)	Neonatal rat ventricle	15	16–18	0.02 Ca^{2+}
Kohlhardt et al. (1987)	Neonatal rat heart	13	19.5 ± 1.0	0.2 Ca^{2+}
Kunze et al. (1985)	Neonatal rat ventricle	20	20	0.02 Ca^{2+}
Nilius (1988)	Guinea pig ventricle	27	22–23	0.1 Ca^{2+}
Nilius (1988)	Guinea pig ventricle	14	22–23	20 Ca^{2+}
Patlak and Ortiz (1985)	Adult rat ventricle	9.8	10	1.8 Ca^{2+}

for rabbit SA node cells, $\gamma_{Ca,L}$ at 50 mM Ba^{2+} in these cells can be estimated from the value of 16 pS at 100 mM Ba^{2+} to be around 9 pS. Cavalié et al. (1983) observed a similar single channel conductance with 50 mM Ba^{2+} or 50 mM Ca^{2+} (Table 1). If, again, the same holds true for rabbit SA node cells, $\gamma_{Ca,L}$ in these cells would be around 9 pS at 50 mM Ca^{2+}. Hagiwara et al. (1988) studied the effect of various extracellular Ca^{2+} concentrations, denoted by $[Ca^{2+}]_e$, on $\gamma_{Ca,L}$. They reported the relationship

$$\gamma_{Ca,L} = \gamma_{Ca,L,max}/(1 + K_m/[Ca^{2+}]_e) \quad (6)$$

with K_m = 3.96 mM. Assuming $\gamma_{Ca,L}$ = 9 pS at $[Ca^{2+}]_e$ = 50 mM, Eq. 6 yields a $\gamma_{Ca,L}$ of 3.3 pS at the normal physiological $[Ca^{2+}]_e$ of 2.0 mM. From this value and the model $\bar{g}_{Ca,L}$ of 36 nS, it follows that $N_{Ca,L}$ is ~11,000.

Applying an analysis of stationary current fluctuations at a membrane potential of −30 mV in small strips of rabbit SA node tissue, Osterrieder et al. (1982) obtained a $\gamma_{Ca,L}$ of 6.50 ± 3.15 pS (mean ± SD, n = 10) at 36°C and 10 mM Ba^{2+}, from which they estimated $\gamma_{Ca,L}$ to be around 4 pS in normal Tyrode's solution. From this, $N_{Ca,L}$ is calculated to be ~9,000, agreeing well with the value derived above. All in all, it seems reasonable to assume $N_{Ca,L}$ = 10,000. Thus, the model $\gamma_{Ca,L}$ amounts to 3.6 pS.

Number of $i_{Ca,T}$ channels

Hagiwara et al. (1988) reported a $\gamma_{Ca,T}$ of 8.5 pS at 37°C in rabbit SA node cells, the extracellular solution containing 100 mM Ba^{2+} as the charge carrier. In guinea pig ventricular cells, Nilius et al. (1985) and Droogmans and Nilius (1989) observed similar values of $\gamma_{Ca,T}$ with equimolar concentrations of Ba^{2+} or Ca^{2+} (Table 1). If the same holds true for rabbit SA node cells, $\gamma_{Ca,T}$ would be around 8.5 pS at 100 mM Ca^{2+} in these cells. Hagiwara et al. (1988) reported an Eq. 6-like relationship between $\gamma_{Ca,T}$ and $[Ca^{2+}]_e$ with a K_m of 0.95 mM. Assuming $\gamma_{Ca,T}$ = 8.5 pS at $[Ca^{2+}]_e$ = 100 mM, this relationship yields a $\gamma_{Ca,T}$ of 5.8 pS at the normal physiological $[Ca^{2+}]_e$ of 2.0 mM. Assuming $\gamma_{Ca,T}$ = 5.8 pS, and the model $\bar{g}_{Ca,T}$ being 25.5 nS, it follows that $N_{Ca,T}$ = 4400.

Number of i_f channels

Carrying out experiments on rabbit SA node cells at 36°C and extracellular K^+ and Na^+ concentrations, denoted by $[K^+]_e$ and $[Na^+]_e$, of 70 mM each, DiFrancesco (1986) found a γ_f of 0.98 pS. Compared with the normal values of 5.4 and 140 mM, respectively, $[K^+]_e$ was high and $[Na^+]_e$ was low. A low $[Na^+]_e$ does not affect the $\bar{i}_f$ slope conductance, but a high $[K^+]_e$ raises it (DiFrancesco et al., 1986). Thus far, no quantitative data on this increase in conductance have become available. Assuming a 2-fold increase, γ_f is ~0.5 pS under normal physiological conditions. Assuming γ_f = 0.5 pS, and the model $\bar{g}_f$ being 12 nS, we obtain N_f = 24,000.

Number of i_K channels

Combining results of his whole cell and single channel experiments on nodal cells isolated from the rabbit heart, Shibasaki (1987) calculated the number of i_K channels per cell as 1054 ± 284 (mean ± SD, n = 13). Therefore, we assume N_K = 1000. From this value and our model $\bar{i}_K$, it follows that γ_K amounts to ~2.9 pS in the membrane potential range of diastolic depolarization.

Number of i_{Na} channels

No data are available on γ_{Na} in SA node cells. Comparing the data obtained from experiments on ventricular cells (Table 1) and keeping in mind that the single channel conductance of cardiac Na^+ channels exhibits a Q_{10} near 1.3 (Kohlhardt, 1990), we feel that it is reasonable to assume γ_{Na} = 20 pS. From this value and the model $\bar{g}_{Na}$ of 12.5 nS, we obtain N_{Na} = 625.

Scaling to membrane capacitance

Our single cell model describes the electrical activity of a 32-pF cell. According to Nakayama et al. (1984), the membrane capacitance (C_m) of nodal cells isolated from the rabbit heart is proportional to membrane area, whereas membrane resistance is inversely proportional to membrane area. Therefore, we assume that the above numbers of ion channels are proportional to C_m. So, when describing the electrical activity of cells with different C_m values, these numbers of ion channels, as well as all current magnitudes, are multiplied by C_m/32 pF, thus scaling them to C_m.

RESULTS AND DISCUSSION

Action potential parameters: experimental observations

Before presenting and discussing model results, we pay attention to experimentally observed fluctuations in action potential parameters of single isolated rabbit SA node cells. Data from cell 910221c1 were used to illustrate essential features of these fluctuations. This particular cell was chosen because its membrane capacitance had been determined and its mean interbeat interval was close to that of our model cell (Table 2).

Coefficient of variation of interbeat interval

Data on fluctuations in IBI of 14 single pacemaker cells isolated from the rabbit SA node are listed in Table 2. All cells were spindle-shaped with a length of 30–60 μm and a width of 7–10 μm. According to Nakayama et al. (1984), membrane capacitance of nodal cells isolated from the rabbit heart normalized to membrane "surface area" amounts to 1.30 ± 0.24 μF/cm² (mean ± SD, n = 18). Thus, one would expect these cells to have C_m values of 10–30 pF. The three C_m values determined were within this range (Table 2).

Table 2 Fluctuations in interbeat interval of single pacemaker cells isolated from the rabbit sinoatrial node: experimental observations*

Experiment	C_m (pF)	IBI (ms)	C_{IBI} (%)
910108c2	23	273 ± 7.7 (n = 100)	2.8
910121c1		378 ± 6.3 (n = 71)	1.7
910212c1		325 ± 6.6 (n = 134)	2.0
910212c2		332 ± 6.2 (n = 135)	1.9
910221c1	20	379 ± 6.3 (n = 105)	1.7
910507c1	22	455 ± 8.1 (n = 64)	1.8
910507c2		399 ± 10.5 (n = 33)	2.6
910507c5		270 ± 5.7 (n = 48)	2.1
910828c2		212 ± 3.9 (n = 39)	1.9
910828c4		313 ± 8.1 (n = 90)	2.6
910925c1		293 ± 6.6 (n = 70)	2.2
911002c1		260 ± 5.9 (n = 65)	2.3
911016c2		238 ± 3.8 (n = 71)	1.6
911017c2		231 ± 3.3 (n = 68)	1.4

* Observations by E. E. Verheijck, A. C. G. van Ginneken, and L. N. Bouman.

Trains of 33–135 action potentials were recorded from each cell. Mean interbeat interval ($\overline{IBI}$) and standard deviation of interbeat interval (σ_{IBI}) were calculated from these recordings. The coefficient of variation of the interbeat interval (C_{IBI}) was calculated according to

$$C_{IBI} = \sigma_{IBI}/\overline{IBI}. \quad (7)$$

Note that C_{IBI} defined this way differs from the coefficient of variation used by Clay and DeHaan (1979), but is similar to the one used by Jongsma and Tsjernina (1982), Clay and DeFelice (1983), and Jongsma et al. (1983, 1987). The standard deviation of IBI increases with increasing $\overline{IBI}$ (Fig. 3 *A*), whereas C_{IBI} appears to be independent of $\overline{IBI}$ (Fig. 3 *B*), in contrast to the findings of Jongsma et al. (1987) that C_{IBI} of single isolated neonatal rat heart cells increases with increasing $\overline{IBI}$. The apparent independence of $\overline{IBI}$ led us to use C_{IBI} as a measure of IBI fluctuations of rabbit SA node cells.

In the 14 cells examined, C_{IBI} ranges from 1.4 to 2.8% (Table 2) and amounts to 2.0% on the average (Fig. 3 *B*). So, beating of rabbit SA node cells is much more regular than that of single isolated embryonic chick ventricular cells or single isolated neonatal rat heart cells, for which C_{IBI}, calculated according to Eq. 7, is ~16% (estimated from Clay and DeHaan, 1979), and ~16% if $\overline{IBI}$ is ~400 ms (Jongsma et al., 1987), respectively.

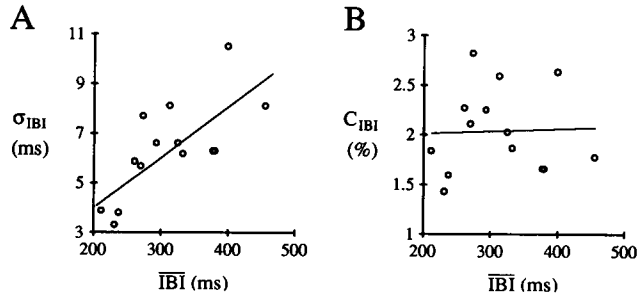

FIGURE 3 Fluctuations in IBI of 14 single isolated rabbit sinoatrial node cells, derived from series of 33–135 consecutive intervals. (*A*) Standard deviation of IBI (σ_{IBI}) as a function of mean interbeat interval ($\overline{IBI}$). The solid line is the linear regression line through (0,0) (r = 0.72). Its slope is 2.0%. (*B*) Coefficient of variation of IBI (C_{IBI}) as a function of $\overline{IBI}$. The solid line is the linear regression line (r = 0.036).

Along with the interbeat interval, seven other action potential parameters were determined (see "Glossary"). Fluctuations in action potential amplitude (APA), action potential duration at 50% repolarization (APD_{50}), action potential duration at 100% repolarization (APD_{100}), MDP, and $\dot{V}_{max}$ were relatively small. Coefficients of variation amounted to ~1, ~2.5, ~4, ~1, and ~1%, respectively. Fluctuations in DDR and TOP, on the other hand, were relatively large, with coefficients of variation of ~15%.

Autocorrelation and distribution of interbeat interval

The most straightforward way, perhaps, to demonstrate IBI fluctuations is to superimpose consecutive action potentials. Superimposed action potentials of cell 910221c1 are depicted in Fig. 4 *A*. Comparing Fig. 4 *A* with Fig. 1 demonstrates that rabbit SA node cells may exhibit a large cell-to-cell variation in action potential parameters.

To test whether interbeat intervals of the action potentials depicted in Fig. 4 *A* were correlated, we calculated the serial correlation coefficient of lag 1–20 from the IBI time series. From the thus obtained autocorrelogram (Fig. 4 *B*) we conclude that consecutive interbeat intervals of cell 910221c1 are not correlated. A similar conclusion was drawn for the remaining 13 cells. A rapid fall to zero in the serial correlation coefficient has previously been found in aggregates of embryonic chick ventricular cells (Guevara, 1984) and neonatal rat heart cells (E. Stutterheim, and H. J. Jongsma, unpublished observations).

Grouping intervals into 5-ms bins, we obtained IBI histograms that had a Gaussian appearance (Fig. 4 *C*). Testing for normality at the 0.05 level of significance using Kolmogorov-Smirnov statistics led to rejection of normality for one cell only (cell 910507c1), whereas moderate p values were obtained for the remaining 13 cells. IBI histograms from clusters of >30 embryonic chick ventricular cells also appeared Gaussian, whereas IBI histograms from smaller clusters and single cells were skewed toward longer intervals (Clay and DeHaan, 1979), just like IBI histograms from single isolated neonatal rat heart cells (Jongsma and Tsjernina, 1982).

Fluctuations in diastolic depolarization rate

Clay and DeHaan (1979) hypothesized that fluctuations in IBI of embryonic chick ventricular cells were brought about by fluctuations in V_m superimposed on the slope of the diastolic depolarization, causing variations in the time it takes for V_m to reach threshold. They noted that this model failed to correspond to reality in several ways, e.g., in not accounting for random variations in threshold. Jongsma and Tsjernina (1982) proposed a similar model to explain IBI

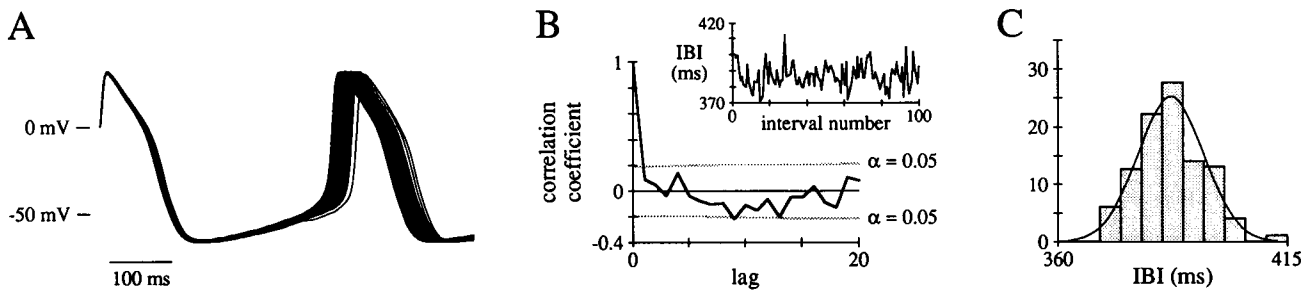

FIGURE 4 Fluctuations in interbeat interval of a single pacemaker cell isolated from the rabbit sinoatrial node. Data from cell 910221c1; number of intervals analyzed = 100. (*A*) Superimposed action potentials. (*B*) Autocorrelogram of the interbeat interval. Confidence limits at the 0.05 level of significance are indicated by dotted lines. The inset shows the time series from which the autocorrelogram was derived. (*C*) Interbeat interval grouped into 5-ms bins. The smooth curve superimposed on the histogram is the normal distribution to which the data were fitted. Mean = 379 ms; SD = 6.4 ms.

fluctuations of single isolated neonatal rat atrial and ventricular cells. Little attention has been paid to IBI fluctuations of single isolated rabbit SA node cells. op 't Hof et al. (1987) attributed these fluctuations to "variability in the second part of diastole."

Let us assume that, in accordance with the above models, IBI fluctuations of single isolated rabbit SA node cells arise from fluctuations in DDR from a fixed MDP toward a fixed TOP. In the 14 cells examined, the coefficient of variation of DDR^{-1} ranges from 10 to 26%. For cell 910221c1 it amounts to 14%. From this figure one would expect the coefficients of variation of IBI-APD_{100} and IBI of this cell to be ~14 and ~6.5%, respectively. The actual figures, however, are 4.8 and 1.7%, respectively. In Fig. 5 *A* it is demonstrated that the actual IBI-APD_{100} is only weakly dependent on DDR^{-1} (Fig. 5 *A*, *circles*), in contrast, of course, to the IBI-APD_{100} expected from the assumption made (Fig. 5 *A*, *squares*).

From the action potential parameters we can discern two relationships that prevent large fluctuations in DDR from inducing large fluctuations in IBI. First, there are large fluctuations in "threshold" that exhibit a clear-cut relation to DDR (Fig. 5 *B*): the higher DDR, the longer the way to threshold (TOP-MDP). MDP is very nearly constant, whereas TOP can be 10–22 mV positive to MDP, with a 17% coefficient of variation. This way, the 14% coefficient of variation of DDR^{-1} is "reduced" to a 4.8% one of IBI-APD_{100}. If APD_{100} were constant, this figure would yield a C_{IBI} of 2.2%. Secondly, there is a negative correlation between APD_{100} and IBI-APD_{100} (Fig. 5 *C*), thus "reducing" C_{IBI} even further to its actual value of 1.7%. Similar relationships were discerned from the action potential parameters of the remaining 13 cells.

Action potential parameters: model results

Now that we have presented and discussed experimental observations of fluctuations in action potential parameters of rabbit SA node cells, we turn to fluctuations in action potential parameters of our stochastic model cell.

Coefficient of variation of interbeat interval

To get an impression of the IBI fluctuations of our standard, 32-pF, model cell, we calculated C_{IBI} from trains of 100 action potentials. Different trains were obtained by setting the seeds of our random number generator to different values. Similar calculations were carried out for 16- and 23-pF model cells. Results are listed in Table 3. Model values of C_{IBI} are quite similar to the ones obtained experimentally (Table 2) and increase slightly with decreasing C_m, i.e., with decreasing numbers of membrane ionic channels (Table 3).

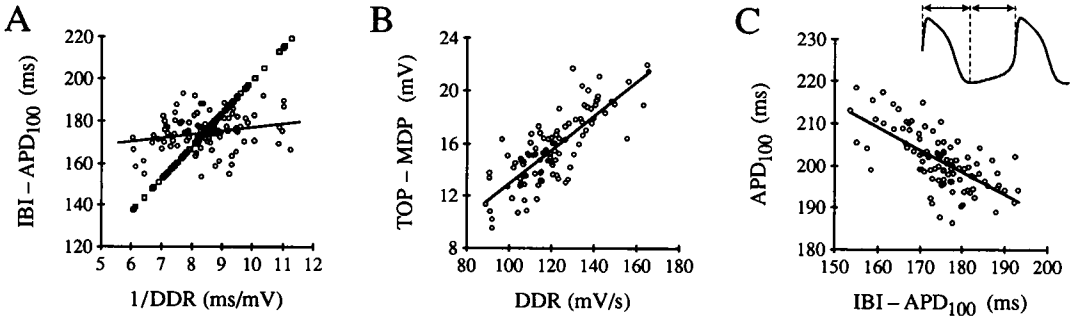

FIGURE 5 Large fluctuations in DDR from MDP toward TOP of single isolated rabbit sinoatrial node cells do not result in large fluctuations in IBI, due to fluctuations in TOP and APD_{100}. Data from cell 910221c1; number of action potentials analyzed = 100. (*A*) Relationship between IBI-APD_{100} and DDR^{-1} (○). The solid line is the linear regression line (r = 0.22). If MDP and TOP are assumed to be constant, a linear relationship between IBI-APD_{100} and DDR^{-1} (□) is expected. (*B*) Relationship between TOP-MDP and DDR. The solid line is the linear regression line (r = 0.80). (*C*) Relationship between APD_{100} and IBI-APD_{100} (*inset*). The solid line is the linear regression line (r = –0.67).

Trains of 100 action potentials appear to be too short to obtain reliable estimates of C_{IBI} (Table 3). Therefore, we calculated C_{IBI} from trains of 1000 action potentials in most cases.

Autocorrelation and distribution of interbeat interval

Fig. 6 *A* was constructed by superimposing 100 consecutive action potentials of our 20-pF model cell. It does not differ from its experimental counterparts (Figs. 1 and 4 *A*) in essential respects. It should, however, be noted that essential features, e.g., fluctuations in TOP, are easily masked by superimposing action potentials when taking the common point on the upstroke of the action potential. Indeed, it was such superimposed action potentials that led op 't Hof et al. (1987) to attribute IBI fluctuations of rabbit SA node cells to "variability in the second part of diastole."

As before, we calculated serial correlation coefficients of lag 1–20 from the IBI time series and constructed the autocorrelogram (Fig. 6 *B*), from which we conclude that consecutive interbeat intervals of our model cell are not correlated. This was confirmed by analyzing trains of 1000 action potentials. This result is not trivial: in some gating processes, e.g., those of i_f and i_K channels, time constants of 100–600 ms are involved, so that a degree of current activation that is high or low by chance may affect several interbeat intervals.

The IBI histogram of our model cell, obtained by grouping intervals into 5-ms bins, has a Gaussian appearance (Fig. 6 *C*). Testing for normality at the 0.05 level of significance using Kolmogorov-Smirnov statistics did not lead to rejection of normality in this particular case, nor did it when trains of 1000 action potentials were analyzed.

Fluctuations in diastolic depolarization rate

Interbeat intervals of our model cell resemble the ones observed experimentally with respect to their coefficient of variation (Tables 2 and 3), their autocorrelation (Figs. 4 *B* and 6 *B*), and their distribution (Figs. 4 *C* and 6 *C*). Also, coefficients of variation of the seven other action potential parameters were well within the range observed experimentally. In particular, DDR and TOP of our 20-pF model cell revealed coefficients of variation >10%.

Table 3 Fluctuations in interbeat interval of single pacemaker cells isolated from the rabbit sinoatrial node: model results*

Run	C_m(pF)	IBI (ms)	C_{IBI} (%)
1	16	387 ± 9.0 (n = 100)	2.3
2	16	389 ± 7.7 (n = 100)	2.0
3	16	386 ± 9.2 (n = 100)	2.4
4	23	388 ± 6.1 (n = 100)	1.6
5	23	388 ± 7.0 (n = 100)	1.8
6	23	387 ± 6.6 (n = 100)	1.7
7	32	389 ± 6.4 (n = 100)	1.6
8	32	387 ± 5.5 (n = 100)	1.4
9	32	388 ± 5.9 (n = 100)	1.5

* The number of membrane ionic channels was assumed to be proportional to membrane capacitance.

The way in which fluctuations in APD_{100}, DDR, and TOP of our model cell "cooperate" to produce relatively small fluctuations in IBI is similar to that set out in Fig. 5 for the experimental case (Fig. 7). The relationship between TOP-MDP and DDR (Fig. 7 *B*) can be explained in terms of i_f activation and i_K deactivation, which both are slow processes. If DDR is relatively low, the membrane potential stays close to MDP during a 150-ms time interval starting at MDP + 1 mV (cf. Fig. 2 *A*). By the end of this time interval, a relatively large amount of i_f channels is activated, whereas a relatively large amount of i_K channels is deactivated. As a consequence, activation of a relatively small amount of $i_{Ca,L}$ channels is sufficient to initiate the upstroke of the action potential, resulting in a takeoff potential that is relatively close to MDP.

The relationship between APD_{100} and IBI-APD_{100} (Fig. 7 *C*) can be explained in terms of i_K activation. If, by chance, a relatively large amount of i_K channels is activated during repolarization of the action potential, this repolarization is relatively fast, resulting in a short APD_{100}. The i_K kinetics are so slow that a relatively large amount of i_K channels is still activated during the next diastolic depolarization, resulting in a relatively low DDR and a relatively long IBI-APD_{100} (Fig. 7 *A*).

Role of various membrane currents

The stochastic behavior of the net membrane current, i_{tot}, and its five gated components during the diastolic depolarization phase of the action potential of our 20-pF model cell is depicted in Fig. 8. The number of i_K channels open decreases from ~400 near MDP to ~120 by the end of the 150-ms time interval. The accompanying increase in i_K is due to an increase in i_K single channel current upon approaching the takeoff potential. The numbers of $i_{Ca,L}$ and i_f channels open increase from 1 to ~30, and from ~50 to ~250, respectively, whereas the numbers of $i_{Ca,T}$ and i_{Na} channels open range between 0 and 4, and 0 and 3, respectively.

Fig. 8 gives an impression of ion channel activity during diastolic depolarization, but it is difficult to draw conclusions from it about the contribution of each gated membrane current to IBI fluctuations. A large contribution is expected if both single channel current and mean channel open time are large, so that opening of a single channel results in a significant change in membrane potential. If, however, single channel currents are large, like $i_{Ca,L}$, $i_{Ca,T}$, and i_{Na}, mean channel open times are small, and conversely, like i_f and i_K (cf. Fig. 8).

To determine the contribution of each gated membrane current to IBI fluctuations, we calculated C_{IBI} from trains of 1000 action potentials of our model cell with only one gated membrane current described stochastically. Calculations were carried out for C_m values of 8–128 pF. Results are shown in Fig. 9, together with C_{IBI} of our model cell with all gated membrane current components described stochasti-

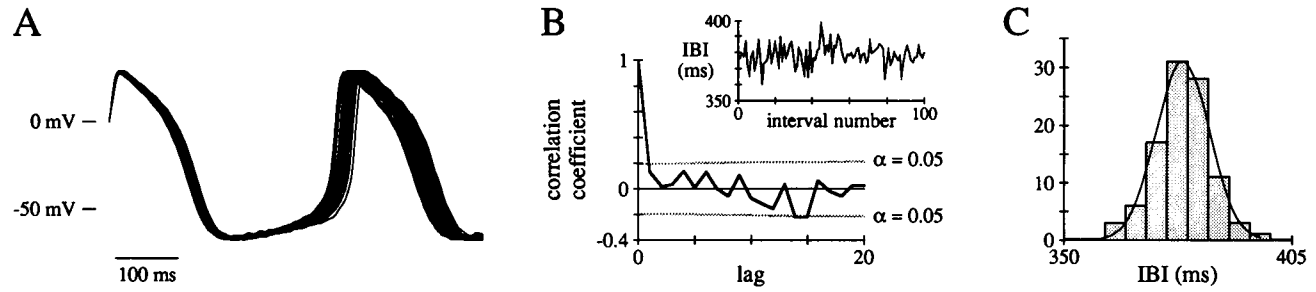

FIGURE 6 Fluctuations in interbeat interval of a 20-pF model rabbit sinoatrial node cell. Number of intervals analyzed = 100. (*A*) Superimposed action potentials. (*B*) Autocorrelogram of the interbeat interval. Confidence limits at the 0.05 level of significance are indicated by dotted lines. The inset shows the time series from which the autocorrelogram was derived. (*C*) Interbeat interval grouped into 5-ms bins. The smooth curve superimposed on the histogram is the normal distribution to which the data were fitted. Mean = 387 ms; SD = 7.9 ms.

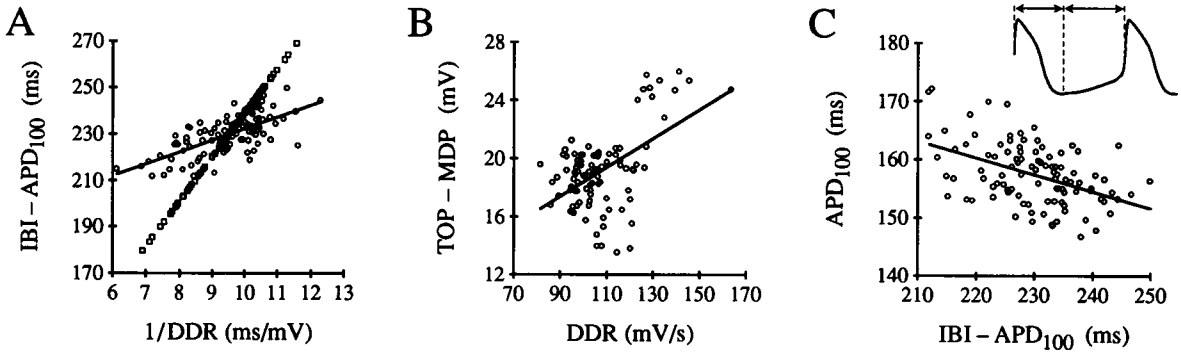

FIGURE 7 Like the experimental case, large fluctuations in DDR from MDP toward TOP of the 20-pF model rabbit sinoatrial node cell do not result in large fluctuations in IBI, due to fluctuations in TOP and APD_{100}. Number of action potentials analyzed = 100. (*A*) Relationship between IBI-APD_{100} and DDR^{-1} (○). The solid line is the linear regression line ($r = 0.68$). If MDP and TOP are assumed to be constant, a linear relationship between IBI-APD_{100} and DDR^{-1} (□) is expected. (*B*) Relationship between TOP-MDP and DDR. The solid line is the linear regression line ($r = 0.53$). (*C*) Relationship between APD_{100} and IBI-APD_{100} (*inset*). The solid line is the linear regression line ($r = -0.45$).

cally. The latter C_{IBI} was almost equal to the root-mean-square of the individual C_{IBI} values of the gated membrane currents. In this respect the gated membrane currents are "independent" sources of "IBI noise." According to Fig. 9, i_K and $i_{Ca,L}$ play an important role in generating this IBI noise.

Data presented in Fig. 9 could be well fitted to the relation $C_{IBI} \sim C_m^{\,s}$ ($r > 0.999$). The slope $s \pm$ SE was -0.52 ± 0.01 if all gated membrane current components were described stochastically. So, C_{IBI} of our model cell is, approximately, inversely proportional to the square root of membrane area or, equivalently, to the square root of the number of ion channels in the cell membrane. This result is similar to the experimental observation of Clay and DeHaan (1979) that C_{IBI} of clusters of embryonic chick ventricular cells is proportional to $N^{-1/2}$, where N is the number of cells in the cluster: these cells are so well coupled that an increase in N may be regarded as an increase in membrane area of a single cell. Furthermore, Clay and DeFelice (1983) obtained a similar relationship between latency fluctuations of nerve membrane patches and patch area in a stochastic version of the Hodgkin and Huxley (1952) model.

The $C_{IBI} \sim A_m^{-1/2}$ relationship should not be regarded as a result of general nature. Skaugen and Walløe (1979), e.g., constructed a stochastic model of a spontaneously firing patch of nerve membrane based upon the Hodgkin and Huxley (1952) model and observed a nonlinear log-log relationship between the standard deviation of the interspike interval and the numbers of potassium and sodium channels in the patch. For pore numbers <10,000 the "slope" was ~ -0.1 for the potassium channels and ~ -0.2 for the sodium channels.

According to Fig. 9, C_{IBI} is related to the numbers of ion channels in the cell membrane. So, one may want to relate experimentally observed differences in C_{IBI} to differences in C_m or magnitudes of membrane currents, as a measure of these numbers of ion channels. No attempts were made to measure individual membrane current components, nor was C_m determined for all cells. So, cell-to-cell variation in IBI fluctuations (Table 2, Fig. 3 *B*) cannot be related to numbers of membrane ionic channels through magnitudes of membrane current components, nor through C_m, from the present experimental data.

Different diastolic depolarization rates

Conceiving diastolic depolarization as a noisy drift of V_m from MDP toward firing threshold, C_{IBI} should be relatively

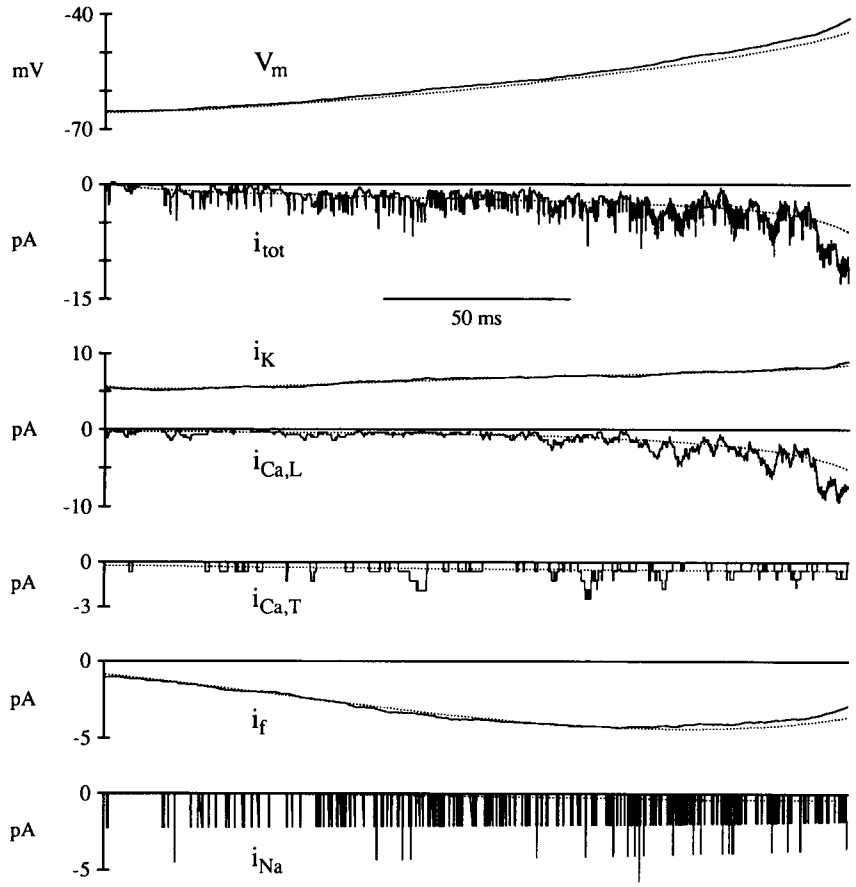

FIGURE 8 Membrane potential, V_m, and net membrane current, i_{tot}, of a 20-pF rabbit sinoatrial node cell during 150 ms of normal spontaneous electrical activity, starting at the maximum diastolic potential, according to the stochastic model (*solid lines*) and the deterministic model (*dotted lines*). The five gated components of i_{tot} are also shown. Note differences in ordinate scales. See "Glossary" for abbreviations.

small in cells with a high DDR (Clay and DeHaan, 1979; Jongsma and Tsjernina, 1982). However, no clear-cut relation between C_{IBI} and DDR was observed in the 14 cells examined here (not shown). In the model, C_{IBI} increases with decreasing DDR, if this decrease is accomplished by lowering the fully activated i_f conductance (Fig. 9, ◇). If, however, both $i_{Ca,L}$ and i_K are scaled, and the sodium-potassium current adjusted properly, to decrease DDR, a decrease in C_{IBI} is observed (not shown). If a constant seal resistance of 5 GΩ is incorporated into the model, DDR increases, but C_{IBI} does not change (see below). So, according to the model, there is no clear-cut relation between C_{IBI} and DDR, either.

Single cells from chick and rat heart

Single isolated embryonic chick ventricular cells are small spherical cells with a membrane surface area of ~300 μm^2 calculated from the diameter of ~10 μm (Clay and DeHaan, 1979; Veenstra, 1990), an input resistance of 1–10 GΩ (Veenstra, 1990), and a C_{IBI} of ~16% (estimated from Clay and DeHaan, 1979). Single isolated neonatal rat heart cells are small spherical cells, too, with a membrane surface area of ~300 μm^2 calculated from the diameter of ~10 μm (Rook et al., 1988) and an input resistance of 2–10 GΩ (Rook et al., 1992). Their C_{IBI} increases with increasing $\overline{IBI}$, but amounts to ~16% if $\overline{IBI}$ is ~400 ms (Jongsma et al., 1987).

The single isolated rabbit SA node cells, data of which were used in this study, had a membrane surface area of ~1500 μm^2. Consequently, their input resistance must have been ~1 GΩ (Nakayama et al., 1984). Their membrane capacitance was ~20 pF (Table 2), ~5 times larger than that of embryonic chick ventricular cells (Veenstra, 1990). So, in terms of membrane area, membrane capacitance, and input resistance, the rabbit SA node cells were ~5 times "larger" than embryonic chick ventricular cells as well as neonatal rat heart cells. From the above C_{IBI} values of 16% and the $C_{IBI} \sim A_m^{-1/2}$ relationship observed experimentally (Clay and DeHaan, 1979) and in this model study (Fig. 9), one would expect that C_{IBI} of rabbit SA node cells were as large as ~7%. As pointed out before, a similar value might be expected from fluctuations in DDR. The true value, however, is ~2% (Fig. 3 *B*), due to the weak correlation between IBI and DDR (cf. Fig. 5). The larger C_{IBI} values of single cells from chick and rat heart point to a stronger correlation between IBI and DDR, as suggested by the good fit of data from embryonic chick ventricular cells to a random walk to threshold model (Clay and DeHaan, 1979).

Background currents

In our model cell, a sodium background current, $i_{b,Na}$, contributes substantially to diastolic depolarization, although it

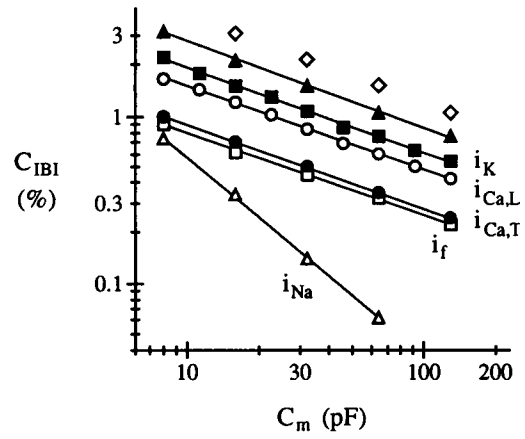

FIGURE 9 Coefficient of variation of interbeat interval (C_{IBI}) as a function of membrane capacitance (C_m), plotted on a double logarithmic scale. The number of ionic channels comprising the cell membrane was assumed to be proportional to C_m. Values were calculated from 1000 consecutive action potentials. Channels described stochastically were $i_{Ca,L}$ channels only (○), $i_{Ca,T}$ channels only (●), i_f channels only (□), i_K channels only (■), i_{Na} channels only (△), or all gated channels (▲). The "all gated channels" simulations were repeated for model cells with the fully activated i_f conductance set to zero, yielding slightly larger C_{IBI} values (◇). Solid lines were obtained by fitting the data to the relation $C_{IBI} \sim C_m^s$ using a linear least-squares method, yielding a slope $s \pm$ SE of -0.50 ± 0.01 for $i_{Ca,L}$, -0.51 ± 0.01 for $i_{Ca,T}$, -0.50 ± 0.01 for i_f, -0.51 ± 0.01 for i_K, -1.19 ± 0.02 for i_{Na}, and -0.52 ± 0.01 if all gated membrane current components were described stochastically ($r > 0.999$).

is not necessary for it to occur (Wilders et al., 1991). A recent study of background current in rabbit SA node cells (Hagiwara et al., 1992) revealed a sodium background current with a current density of 0.73 ± 0.21 pA/pF (mean $\pm$ SD, $n = 71$) at -50 mV, close to our model value of 0.60 pA/pF. If $i_{b,Na}$ flows through some unknown "background channels" that flip randomly between an open and a closed state, it may contribute substantially to fluctuations in interbeat interval. Therefore, we investigated the effects of describing $i_{b,Na}$ as a current flowing through N identical, independent ion channels, the kinetics of which are given by V_m-independent Hodgkin and Huxley (1952) type rate constants α and β.

Consider $i_{b,Na}$ as a gated membrane current with fully activated conductance $\bar{g}$ resulting from a population of N identical, independent ion channels with open probability p, single channel conductance γ, and reversal potential V_{rev}. Under steady-state conditions, the variance of the current flowing through the channels, i, is given by

$$\sigma_i^2 = \sigma_n^2[\gamma(V_m - V_{rev})]^2, \quad (8)$$

where σ_n^2 is the variance of the number of open channels, n, which is that of a binomial distribution:

$$\sigma_n^2 = Np(1 - p), \quad (9)$$

where $N = \bar{g}/\gamma$. Of course, the average $i_{b,Na}$ conductance must equal the $i_{b,Na}$ conductance $g_{b,Na}$ of the deterministic model. So, we have $\bar{g} = g_{b,Na}/p$ with $g_{b,Na} = 0.15$ nS. Combining Eqs. 8 and 9 and substituting $g_{b,Na}/p$ for $\bar{g}$ and V_{Na} for V_{rev}, we arrive at

$$\sigma_{i_{b,Na}}^2 = g_{b,Na}\,\gamma(1 - p)(V_m - V_{Na})^2, \quad (10)$$

with $N = g_{b,Na}/(p\gamma)$. According to Eq. 10, a substantial contribution to fluctuations in i_{tot} is expected if γ is large and p is small. If gated background channels exist, their single channel conductance must be small. Otherwise, their single channel activity would have been observed experimentally.

With $\gamma = 0.5$ pS and $p = 0.1$, and, consequently, $N = 3000$, Eq. 10 yields $\sigma_{ib,Na}$ values around 0.1 pA in the potential range of diastolic depolarization, which is, e.g., about 4 times smaller than the steady-state σ_i of $i_{Ca,T}$ calculated from Eqs. 8 and 9. From this, it should not be concluded that the contribution of $i_{b,Na}$ to IBI fluctuations is small, because this contribution may depend strongly on the mean channel open time or, equivalently, the time constant of channel gating τ. Therefore, we incorporated the stochastic behavior of $i_{b,Na}$ channels, with $\alpha = p/\tau$ and $\beta = (1 - p)/\tau$, into our deterministic 32-pF model cell and calculated C_{IBI} from trains of 1000 action potentials for τ values of 1–300 ms. Results show that gating of $i_{b,Na}$ channels may produce C_{IBI} values >1.5% if τ is between 40 and 200 ms (Fig. 10, *circles*). For small τ values, however, C_{IBI} is small too and is proportional to $\tau^{1/2}$. The $C_{IBI} \sim \tau^{1/2}$ relationship is similar to the $C_{IBI} \sim N^{-1/2}$ relationship of Fig. 9: both τ^{-1} and N are linearly related to the expected number of channel openings and closures occurring during an action potential.

From Eq. 10, one may hypothesize that C_{IBI} decreases by a factor of 1.5 if p is set to 0.6 instead of 0.1. Repeating our calculations with $\gamma = 0.5$ pS and $p = 0.6$, and, consequently, $N = 500$, confirmed this hypothesis (Fig. 10, *squares*). One may also hypothesize that the latter C_{IBI} values double if γ is set to 2 pS instead of 0.5 pS, which was confirmed when we repeated our calculations with $\gamma = 2$ pS and $p = 0.6$, and, consequently, $N = 125$ (Fig. 10, *triangles*).

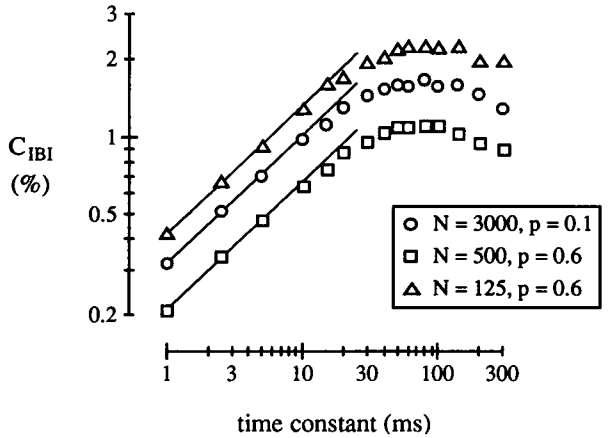

FIGURE 10 Fluctuations in interbeat interval due to gating of the background sodium current ($i_{b,Na}$): coefficient of variation of interbeat interval (C_{IBI}) as a function of the time constant of the gating process (τ), plotted on a double logarithmic scale. Channel gating is described by a simple, voltage-independent two-state first-order process. The number of $i_{b,Na}$ channels (N) and the single channel open probability (p) were 3000 and 0.1 (○), 500 and 0.6 (□), or 125 and 0.6 (△), respectively. Solid lines represent the relation $C_{IBI} \sim \tau^{1/2}$.

If the calcium background current, $i_{b,Ca}$, was described stochastically, the results obtained were qualitatively similar to those presented in Fig. 10 for $i_{b,Na}$, but the maximum C_{IBI} values attained were ~1.7 times smaller. A small potassium background current, $i_{b,K}$, was incorporated into our model to account for the small amount of i_{K1} channels observed experimentally in rabbit SA node cells. The i_{K1} channels are gated channels, but their kinetics are so fast that i_{K1} behaves like a time-independent current in SA node cells. Because i_{K1} kinetics are extremely fast, the contribution of $i_{b,K}$ to fluctuations in interbeat interval is negligible (not shown). We assumed that the stochasticity of other processes, like the sodium-calcium exchange and the sodium-potassium pump, play a minor role in generating fluctuations in interbeat interval.

Rectification of potassium currents

Unlike other currents, both i_K and i_{K1} show inward rectification. As explained before, no attempts were made to incorporate gating of i_{K1} channels into the model, so that $i_{b,K}$ is a time-independent (background) current showing inward rectification. Similarly, inactivation of i_K channels, accounting for their inward rectification (Shibasaki, 1987), was not incorporated. This inactivation is so fast that, for our purposes, it is sufficient to assume that i_K rectification lies in the single channel conductance itself.

Seal leakage current

In 25 rabbit SA node cells, DiFrancesco (1991) observed pipette seal resistances of 2–12 GΩ, with a mean value of 5.1 GΩ. So, seal leakage current may be as large as 5–30 pA in the membrane potential range of diastolic depolarization, so that fluctuations in seal resistance may have considerable effects on fluctuations in IBI.

Incorporation of a constant seal resistance of 5 GΩ into our stochastic model led to an increase in mean DDR and a decrease in mean IBI, whereas C_{IBI} did not change. Seal resistance was allowed to fluctuate around 5 GΩ, say between 4 and 6 GΩ, in small steps by modeling it as a conductance formed by 100 parallel 4-pS "channels" exhibiting V_m-independent Hodgkin and Huxley (1952) type kinetics with an open probability of 0.5 and time constant τ. With all gated channels described stochastically and a constant seal resistance of 5 GΩ, our 32-pF model cell exhibits a C_{IBI} of 1.5%. If, however, seal resistance is allowed to fluctuate, C_{IBI} values of 1.9 and 2.5% are observed, τ amounting to 10 and 100 ms, respectively. Repeating our simulations with 10 parallel 40-pS channels, these values were 2.6 and 4.9%, respectively. The largest C_{IBI} value observed experimentally was only 2.8% (Table 2). Therefore, we speculate that, in the experiments, fluctuations in seal resistance were either small and fast, so that their contribution to IBI fluctuations was only moderate, or large and slow, so that they were accompanied by apparent artifacts in action potential parameters and the experiment was discarded.

Full activation

A general assumption in analyzing voltage clamp data from whole cell experiments is that all channels are in their open state if activation is maximal. In accordance with this assumption, the activation gating variable at this level of activation is set to 1, expressing that all channels are open. When constructing our model, it was assumed that all gating variables saturate at 1. There is, however, experimental evidence from single channel experiments that this assumption need not be true. Maximal activation of $i_{Ca,L}$ channels in guinea pig myocytes, e.g., may saturate at 0.4–0.6 (Cavalié et al., 1983). Model results may change if some saturation level δ, $0 < \delta < 1$, instead of 1 is assumed. Then, the single channel open probability p, the fully activated conductance $\bar{g}$, and the total number of channels N have to be replaced by δp, $\bar{g}/\delta$, and N/δ, respectively. Substituting N/δ for N and δp for p, Eq. 9 changes to

$$\sigma_n^2 = Np(1 - \delta p)$$

So, under steady-state conditions, σ_n increases with decreasing δ. The increase in σ_n, however, is small if p is small: for $\delta = 0.5$, it is <10% if p is <0.3. For all gated membrane currents, single channel open probability is <0.3 in the membrane potential range of diastolic depolarization. From this, one may expect that the effects of saturation at a level <1 on C_{IBI} are small. Indeed, the saturation level of any gating variable could be set to 0.5 without increasing C_{IBI}, determined from trains of 1000 action potentials as before, by more than 3%.

Drawing lifetimes

Throughout, Eq. 1 was used to draw lifetimes T of the membrane state. One may, however, argue that the "ensemble rate constant" λ is a parametric function of time through its dependence on membrane potential, V_m, and that, therefore, T should be determined from

$$\int_0^T \lambda[V_m(t)]\, dt = -\log r$$

(Clay and DeFelice, 1983; van Meerwijk, 1988). Generally, T was very small in our simulations, due to the large number of channels in the model cell membrane, so that ΔV_m, i.e., the change in V_m during T, was very small too. As explained before, a V_m-dependent upper limit Δt_{max} on the integration time step Δt was introduced. This ensured that ΔV_m was small at all times, so that Eq. 12 reduced to the much simpler Eq. 1. A more detailed discussion of this issue was presented by Skaugen and Walløe (1979).

In preliminary simulations, we used a FORTRAN subroutine that was based on Eq. 12 to draw lifetimes (van Meerwijk, 1988). The results obtained were not different from those presented here, but computational speed was ~20 times lower.

This study was supported by the Netherlands Organization for Scientific Research (NWO) through the Foundation for Biophysics (NWO-SvB grant 810–406–151).We thank Drs. E. E. Verheijck, A. C. G. van Ginneken, and L. N. Bouman for providing us with experimental data.

REFERENCES

Blair, E. A., and J. Erlanger. 1932. Responses of axons to brief shocks. *Proc. Soc. Exp. Biol. Med.* 29:926–927.

Cachelin, A. B., J. E. de Peyer, S. Kokubun, and H. Reuter. 1983. Sodium channels in cultured cardiac cells. *J. Physiol. (Lond.).* 340:389–402.

Cavalié, A., R. Ochi, D. Pelzer, and W. Trautwein. 1983. Elementary currents through Ca^{2+} channels in guinea pig myocytes. *Pflügers Arch. Eur. J. Physiol.* 398:284–297.

Clay, J. R., and L. J. DeFelice. 1983. Relationship between membrane excitability and single channel open-close kinetics. *Biophys. J.* 42: 151–157.

Clay, J. R., and R. L. DeHaan. 1979. Fluctuations in interbeat interval in rhythmic heart-cell clusters. *Biophys. J.* 28:377–390.

DeFelice, L. J., and J. R. Clay. 1983. Membrane current and membrane potential from single-channel kinetics. *In* Single-Channel Recording. B. Sakmann and E. Neher, editors. Plenum Publishing Corp., New York. 323–342.

Derksen, H. E., and A. A. Verveen. 1966. Fluctuations of resting neural membrane potential. *Science (Wash. DC)* 151:1388–1389.

DiFrancesco, D. 1986. Characterization of single pacemaker channels in cardiac sino-atrial node cells. *Nature (Lond.).* 324:470–473.

DiFrancesco, D. 1991. The contribution of the 'pacemaker' current (i_f) to generation of spontaneous activity in rabbit sino-atrial node myocytes. *J. Physiol. (Lond.)* 434:23–40.

DiFrancesco, D., A. Ferroni, M. Mazzanti, and C. Tromba. 1986. Properties of the hyperpolarizing-activated current (i_f) in cells isolated from the rabbit sino-atrial node. *J. Physiol. (Lond.).* 377:61–88.

Droogmans, G., and B. Nilius. 1989. Kinetic properties of the cardiac T-type calcium channel in the guinea-pig. *J. Physiol. (Lond.).* 419: 627–650.

Guevara, M. R. 1984. Chaotic cardiac dynamics. Ph.D. thesis. McGill University, Montreal, Canada.

Hagiwara, N., H. Irisawa, and M. Kameyama. 1988. Contribution of two types of calcium currents to the pacemaker potentials of rabbit sino-atrial node cells. *J. Physiol. (Lond.).* 395:233–253.

Hagiwara, N., H. Irisawa, H. Kasanuki, and S. Hosada. 1992. Background current in sino-atrial node cells of the rabbit heart. *J. Physiol. (Lond.).* 448:53–72.

Hamill, O. P., A. Marty, E. Neher, B. Sakmann, and F. J. Sigworth. 1981. Improved patch-clamp techniques for high-resolution current recording from cells and cell-free membrane patches. *Pflügers Arch. Eur. J. Physiol.* 391:85–100.

Hodgkin, A. L., and A. F. Huxley. 1952. A quantitative description of membrane current and its application to conduction and excitation in nerve. *J. Physiol. (Lond.).* 117:500–544.

Horn, R., and A. Marty. 1988. Muscarinic activation of ionic currents measured by a new whole-cell recording method. *J. Gen. Physiol.* 92: 145–159.

Irisawa, H., H. F. Brown, and W. R. Giles. 1993. Cardiac pacemaking in the sinoatrial node. *Physiol. Rev.* 73:197–227.

Jongsma, H. J., and L. Tsjernina. 1982. Factors influencing regularity and synchronisation of beating of tissue cultured heart cells. *In* Cardiac Rate and Rhythm. L. N. Bouman, and H. J. Jongsma, editors. Martinus Nijhoff, London. 397–414.

Jongsma, H. J., M. Masson-Pévet, and L. Tsjernina. 1987. The development of beat-rate synchronization of rat myocyte pairs in cell culture. *Basic Res. Cardiol.* 82:454–464.

Jongsma, H. J., L. Tsjernina, and J. de Bruijne. 1983. The establishment of regular beating in populations of pacemaker heart cells: a study with tissue-cultured rat heart cells. *J. Mol. Cell. Cardiol.* 15:123–133.

Kohlhardt, M. 1990. Different temperature sensitivity of cardiac Na^+ channels in cell-attached and cell-free conditions. *Am. J. Physiol.* 259: C599-C604.

Kohlhardt, M., U. Fröbe, and J. W. Herzig. 1987. Properties of normal and non-inactivating single cardiac Na^+-channels. *Proc. R. Soc. Lond. B Biol. Sci.* B232:71–93.

Kunze, D. L., A. E. Lacerda, D. L. Wilson, and A. M. Brown. 1985. Cardiac Na currents and the inactivating, reopening, and waiting properties of single cardiac Na channels. *J. Gen. Physiol.* 86:691–719.

Lecar, H., and R. Nossal. 1971a. Theory of threshold fluctuations in nerves. I. Relationships between electrical noise and fluctuations in axon firing. *Biophys. J.* 11:1048–1067.

Lecar, H., and R. Nossal. 1971b. Theory of threshold fluctuations in nerves. II. Analysis of various sources of membrane noise. *Biophys. J.* 11: 1068–1084.

Nakayama, T., Y. Kurachi, A. Noma, and H. Irisawa. 1984. Action potential and membrane currents of single pacemaker cells of the rabbit heart. *Pflügers Arch. Eur. J. Physiol.* 402:248–257.

Nilius, B. 1988. Calcium block of guinea-pig heart sodium channels with and without modification by the piperazinylindole DPI 201–206. *J. Physiol. (Lond.).* 399:537–558.

Nilius, B., P. Hess, J. B. Lansman, and R. W. Tsien. 1985. A novel type of cardiac calcium channel in ventricular cells. *Nature (Lond.).* 316: 443–446.

op 't Hof, T., A. C. G. van Ginneken, L. N. Bouman, and H. J. Jongsma. 1987. The intrinsic cycle length in small pieces isolated from the rabbit sinoatrial node. *J. Mol. Cell. Cardiol.* 19:923–934.

Osterrieder, W., Q.-F. Yang, and W. Trautwein. 1982. Conductance of the slow inward channel in the rabbit sinoatrial node. *Pflügers Arch. Eur. J. Physiol.* 394:85–89.

Patlak, J. B., and M. Ortiz. 1985. Slow currents through single sodium channels of the adult rat heart. *J. Gen. Physiol.* 86:89–104.

Reuter, H., C. F. Stevens, R. W. Tsien, and G. Yellen. 1982. Properties of single calcium channels in cardiac cell culture. *Nature (Lond.).* 297: 501–504.

Rook, M. B., H. J. Jongsma, and A. C. G. van Ginneken. 1988. Properties of single gap junctional channels between isolated neonatal rat heart cells. *Am. J. Physiol.* 255:H770-H782.

Rook, M. B., A. C. G. van Ginneken, B. de Jonge, A. El Aoumari, D. Gros, and H. J. Jongsma. 1992. Differences in gap junction channels between cardiac myocytes, fibroblasts and heterologous pairs. *Am. J. Physiol.* 263: C959-C977.

Shibasaki, T. 1987. Conductance and kinetics of delayed rectifier potassium channels in nodal cells of the rabbit heart. *J. Physiol. (Lond.).* 387: 227–250.

Skaugen, E., and L. Walløe. 1979. Firing behaviour in a stochastic nerve membrane model based upon the Hodgkin-Huxley equations. *Acta Physiol. Scand.* 107:343–363.

van Ginneken, A. C. G., and W. R. Giles. 1991. Voltage clamp measurements of the hyperpolarization-activated inward current I_f in single cells from rabbit sino-atrial node. *J. Physiol. (Lond.)* 434:57–83.

van Meerwijk, W. P. M. 1988. Qualitative models for cardiac pacemakers and their interaction. Ph.D. thesis. University of Leiden, The Netherlands. 114 pp.

Veenstra, R. D. 1990. Voltage-dependent gating of gap junction channels in embryonic chick ventricular cell pairs. *Am. J. Physiol.* 258:C662-C672.

Verheijck, E. E., J. Bourier, A. C. G. van Ginneken, and L. N. Bouman. 1992. Distribution and electrical activity of cell types in the rabbit sino-atrial node. *Pflügers Arch. Eur. J. Physiol.* 420:R88. (Abstr.)

Verveen, A. A., and H. E. Derksen. 1965. Fluctuations in membrane potential of axons and the problem of coding. *Kybernetik* 2:152–160.

Victorri, B., A. Vinet, F. A. Roberge, and J.-P. Drouhard. 1985. Numerical integration in the reconstruction of cardiac action potentials using Hodgkin-Huxley-type models. *Comp. Biomed. Res.* 18:10–23.

Wichmann, B. A., and I. D. Hill. 1982. An efficient and portable pseudo-random number generator. *Appl. Stat.* 31:188–190.

Wilders, R. 1993. From single channel kinetics to regular beating: a model study of cardiac pacemaker activity. Ph.D. thesis. University of Amsterdam, The Netherlands. 149 pp.

Wilders, R., H. J. Jongsma, and A. C. G. van Ginneken. 1991. Pacemaker activity of the rabbit sinoatrial node: a comparison of mathematical models. *Biophys. J.* 60:1202–1216.